Heliyon 10 (2024) e24579

Contents lists available at ScienceDirect

Heliyon

journal homepage: www.cell.com/heliyon

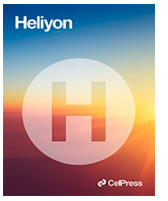

Research article

HO-1 attenuates testicular ischaemia/reperfusion injury by activating the phosphorylated C-jun-miR-221/222-TOX pathway

Bo Xie [a,1], Bing Cheng [b,1], Lugeng He [a], Yunfu Liu [a], Ning He [a,*]

[a] Department of Urology, The First Affiliated Hospital, Zhejiang University School of Medicine, Hangzhou, Zhejiang, 310000, PR China
[b] Department of Department of Geriatric Medicine, Shulan (Hangzhou) Hospital, Zhejiang Shuren University Shulan International Medical College, Hangzhou, Zhejiang, 310000, PR China

ARTICLE INFO

Keywords:
Heme oxygenase (HO-1)
Knockout rats
miR-221/222
c-Jun
Testicular ischaemia/reperfusion
Gene sequencing

ABSTRACT

Aims: Heme oxygenase (HO-1) affords protection against ischaemia/reperfusion (I/R) injury; however, its effects on testicular I/R injury remain poorly explored. Herein, we aimed to examine the effects of HO-1 on testicular I/R injury and elucidate the underlying mechanism.
Methods: Using the TALEN technique, we knocked out the HO-1 gene from rats. *In vivo*: Thirty hmox+/+ and 30 hmox−/− rats were randomly assigned to six groups: sham-operated (sham), I/R (the left testicle torsion/detorsion) 0 d,I/R 1d, I/R 3d, I/R 7d and I/R 28d. *In vitro*: GC-1 were suffered from: control,H/R (oxygen-deprivation/reoxygenation),H/R + HO-1 siRNA,H/R + c-Jun siRNA or H/R + HO-1 siRNA + c-jun.We performed immunofluorescence and immunohistochemistry experiments to detect HO-1 nuclear translocation. Flow cytometry was used to detect cell apoptosis and analyse the cell cycle. High-resolution miRNA, mRNA sequencing, reverse transcription-quantitative PCR, and western blotting were performed to identify testicular I/R injury-related genes strongly conserved in HO-1 knockout rats. A double luciferase reporter assay was performed to verify the relationship between C-jun and miR-221/222.
Main findings: In vivo, HO-1 improved the pathological damage induced by testicular I/R. In GC-1 cells, we confirmed the nuclear translocation of HO-1 and its protective effect against hypoxia/reoxygenation (H/R) damage. Accordingly, HO-1 protein itself, rather than heme metabolites, might play a key role in testicular I/R. Gene sequencing was performed to screen for miR221/222 and its downstream gene, thymocyte selection-associated high mobility group box (TOX). HO-1 increased c-Jun phosphorylation in the H/R group, knocked down c-Jun in GC-1 cells, and decreased miR-221/222 expression. Inhibition of HO-1 expression decreased the expression of c-Jun and miR-221/222, which was rescued by adding c-Jun. Dual-luciferase reporter assay confirmed the interaction between c-Jun and miR-221/222.
Conclusions: HO-1 could exert a protective effect against testicular I/R via the phosphorylated c-Jun-miR-221/222-TOX pathway.

* Corresponding author.
E-mail addresses: zdyyxb@zju.edu.cn (B. Xie), medicinecheng@126.com (B. Cheng), fengyuzhe88@zju.edu.cn (L. He), liuyunfu@hotmail.com (Y. Liu), medicinehe@zju.edu.cn (N. He).
[1] The first two authors contribute equally to the paper.

https://doi.org/10.1016/j.heliyon.2024.e24579
Received 4 August 2023; Received in revised form 29 December 2023; Accepted 10 January 2024
Available online 17 January 2024
2405-8440/© 2024 The Authors. Published by Elsevier Ltd. This is an open access article under the CC BY-NC-ND license (http://creativecommons.org/licenses/by-nc-nd/4.0/).

1. Introduction

Testicular torsion is a common emergency in urology and is caused by the rotation of the vascular pedicle, resulting in testicular necrosis, loss of spermatogenesis, and, most importantly, unavoidable orchiectomy [1]. Surgery is the main option to correct testicular torsion, however, there is a literature regarding manual detorsion in the setting of limited operating room availability or at presentation in the emergency department so as to turn an emergent case into an elective surgery [2,3]. Conservative surgical management, including the derotation of the affected tissue to restore testicular blood flow, is one strategy for early treatment. Testicular torsion and detorsion are the primary causes of testicular ischaemia/reperfusion (I/R) injury [4]. Therefore, elucidating the underlying mechanisms is critical to comprehensively clarify the progression of testicular I/R injury, as well as to identify effective therapeutic targets.

Heme oxygenase (HO-1) is a commonly expressed, inducible enzyme that degrades heme into carbon monoxide (CO), bilirubin, and Fe^{2+}. HO-1 participates in the maintenance of cellular homeostasis and plays a crucial role in protecting organs and tissues from I/R injury by reducing oxidative damage, inhibiting apoptosis, and attenuating inflammatory response [5]. Ferroptosis can be suppressed via Nrf2 by regulating HO-1, which may afford a potential therapeutic strategy for protection against acute lung injury due to intestinal ischaemia reperfusion [6]. In addition, etomidate was shown to attenuate ferroptosis in myocardial I/R via the Nrf2/HO-1 pathway in rats [7]. Kojiro et al. have revealed that HO-1 regulates macrophage activation and hepatocyte death in hepatic I/R injury via the sirtuin1-p53 signalling network [8]. The antioxidant effect of HO-1 has been attributed to the catabolism of free heme, and several studies have shown that free heme is primarily produced via the oxidation of haemoglobin. Free heme can then be used in a Fenton reaction to produce toxic hydroxyl radicals released by hydrogen peroxide, potentially damaging DNA and proteins and leading to programmed cell apoptosis. Thus, HO-1-mediated degradation of free heme restricts the subsequent production of pro-oxidants and cytotoxic substances [9]. The mechanisms underlying the role of HO-1 in I/R remain poorly clarified. Moreover, it is yet to be established whether the HO-1 protein itself or heme metabolites play an important role in I/R injury. In particular, few studies have explored the function of HO-1 in testicular I/R injury.

Therefore, we used gene sequencing, biosynthesis analysis, and reverse transcription (RT)- quantitative PCR to screen miR-221/222 and downstream gene-thymocyte selection associated high mobility group box (TOX) related to testicular I/R injury in HO-1 knockout ($hmox^{-/-}$) rats to elucidate the underlying mechanism. MicroRNAs (miRNAs) are a class of small noncoding RNAs that regulate gene expression after transcription by binding to the 3'utr of the target gene messenger RNAs (mRNAs), resulting in mRNA degradation and/or translational repression. Growing evidence suggests that miRNAs play a role in I/R [10,11]. c-Jun has been associated with the activation of miR-221/222 in prostate cancer and glioblastoma [12]. Combined with the above theoretical basis, we speculated that HO-1 could activate miR-221/222 by interacting with phosphorylated c-Jun in testicular I/R injury to provide a new therapeutic target.

2. Material and methods

2.1. Animals and study design

We used adult male Sprague Dawley rats (250–300 g) maintained in environmentally controlled animal facilities. All experiments were approved by the Animal Care and Use Committee of the First Affiliated Hospital, School of Medicine, Zhejiang University, China. The ethics approval number is 2023–1332. All procedures were performed in strict accordance with the guidelines for laboratory animals and in accordance with the Animal Research: Reporting of In Vivo Experiments (ARRIVE) Guidelines (https://www.nc3rs.org.uk/arrive-guidelines).

In vivo: Thirty $hmox^{+/+}$ and 30 $hmox^{-/-}$ rats were randomly assigned to six groups: sham-operated group (sham), I/R 0 d group,I/R 1d group, I/R 3d group, I/R 7d group and I/R 28d group (n = 5 animals per group). Six $hmox^{+/+}$ rats were randomly assigned to two groups: I/R 0 h group, I/R 1h group (n = 3 animals per group). Furthermore, animals were subjected to the following procedures: following anesthesia induction, the left testicle of rats was twisted clockwise 720°and fixed to the scrotal skin with silk thread (11/0 noninvasive suture, totally 60 uesed). After 2 h of torsion, the testes were allowed to return to their natural position for 0, 1 h or 0, 1, 3, 7, or 28 days; animals were sacrificed after the predetermined period. In the sham group, the testes were positioned through a left scrotal incision without torsion. A total of 2 mL of plasma samples were collected at 0, 1, 3, 7, or 28 days after I/R and at 0 day in the sham group for the analysis of testosterone and follicular stimulating hormone (FSH). The left testicles partial tissues were obtained for Western Blotting collected at 0, 1, 3, 7, or 28 days after I/R and at 0 day in the sham group. And the left testicles partial tissues were fixed in 10 % neutral formalin at 0, 1, and 3 days after I/R and at 0 day in the sham group for histologic analyses, or at 0 and 1 h after I/R for immunohistochemical analyses. Three $hmox^{+/+}$ and 3 $hmox^{-/-}$ rats were suffered from I/R 3d as described above and the left testicles partial tissues were obtained for High-resolution miRNA sequencing. Five $hmox^{+/+}$ and 5 $hmox^{-/-}$ rats were suffered from I/R 3d as described above and the left testicles partial tissues were obtained for Western Blotting of HO-1 and RT-qPCR of miR-221–3p, miR-222–3p, miR125b-2-3p, miR200a-5p, miR429, ATPase phospholipid transporting 8A2 (ATPBA2), TOX, family with sequence similarity 196, member B (FAM196B), solute carrier family 4 member 4 (SLC4A4), and folliculin-interacting protein 2 (FNIP2).

2.2. Generation and validation of TALEN-mediated HO-1 knockout rats

Talen-mediated HO-1 knockout rats were obtained from Beijing View Solid Biotechnology Co., Ltd. The TALEN structures in TALEN-L and TALEN-R expression vectors were prepared using the Hispee plasmid Midi kit. The vectors were linearised using the *Not*I software. TALEN-L and TALEN-R mRNAs were transcribed using the T7 promoter. TALEN-L and TALEN-R mRNAs in M2 medium were

injected into fertilised eggs (n = 120) using a FemtoJet microoperator. After microinjection, fertilised eggs were transferred to pseudopregnant females. Tail-derived DNA from 2-week-old rats was genotyped using PCR products amplified using the following primers: HO-1-T4 sense (TTGACAGCTGGGCTGAAATGCAC) and HO-1-T4 antibody (TTCTGCGCAATCTTCTTCAGGAC). Next, a 507-bp DNA fragment was amplified to confirm the HO-1 mutant allele and identify frameshift mutations by PCR sequencing; mutant rats were mated with wild-type rats to obtain heterozygotes, and heterozygous rats were mated to obtain homozygous rats. PCR was performed on the genomic DNA of rats, the PCR products were sequenced directly, and the mutation was determined by analyzing the sequencing peak type. The sequencing peak diagram shows a single peak, indicating homozygote. Through peak shape analysis, the DNA sequence of the mutant (peak shape indicated by the red arrow) can be analysed, and compared with the DNA sequence of the wild type, it is found that, for example, the rat (Number:Hmox1-6x13-35#)as shown in Fig. 1C lacks 11 bases before CACTCTACTT, and the A before CTCTACTTC of the two chains is mutated to G. Frameshift mutation occurs. According to the above sequence analysis, the rat (Number:HMOX1-6X13-35#) strain is A homozygous Hmox1 frameshift mutant with 11 bases missing before CACTCTACTT, and the A mutation before two chains of CTCTACTTC is G.

2.3. Cell culture conditions

GC-1 (the mouse spermatogonial cell line), GC-2 (the mouse spermatocyte cell line), TM3 (the mouse Leydig cell line), and TM4 (the mouse Sertoli cell line) were purchased from Shanghai Institutes for Biological Sciences (Shanghai, China). Cells were grown in a 5 % CO_2 humidified atmosphere at 37 °C in 75-cm^2 tissue culture flasks.

2.4. Cell hypoxic/reoxygenation (H/R) model

GC-1,GC-2, TM3 and TM4 was cultured under hypoxic conditions in a modular culture chamber (Billumps-Rothenberg, Del Mar, CA, USA) according to the manufacturer's protocol. GC-1 cells were placed in a chamber at 37 °C, rinsed with a mixture of 94 % N_2, 5 % CO_2, and 1 % O_2 for 24 h (oxygen-serum deprivation, ischaemic cells) [13]. Next, repeated hypoxic cultures were returned to the normoxic incubator and serum-containing medium for reoxygenation for 6 h; the control group comprised GC-1 cells cultured under normoxic conditions.

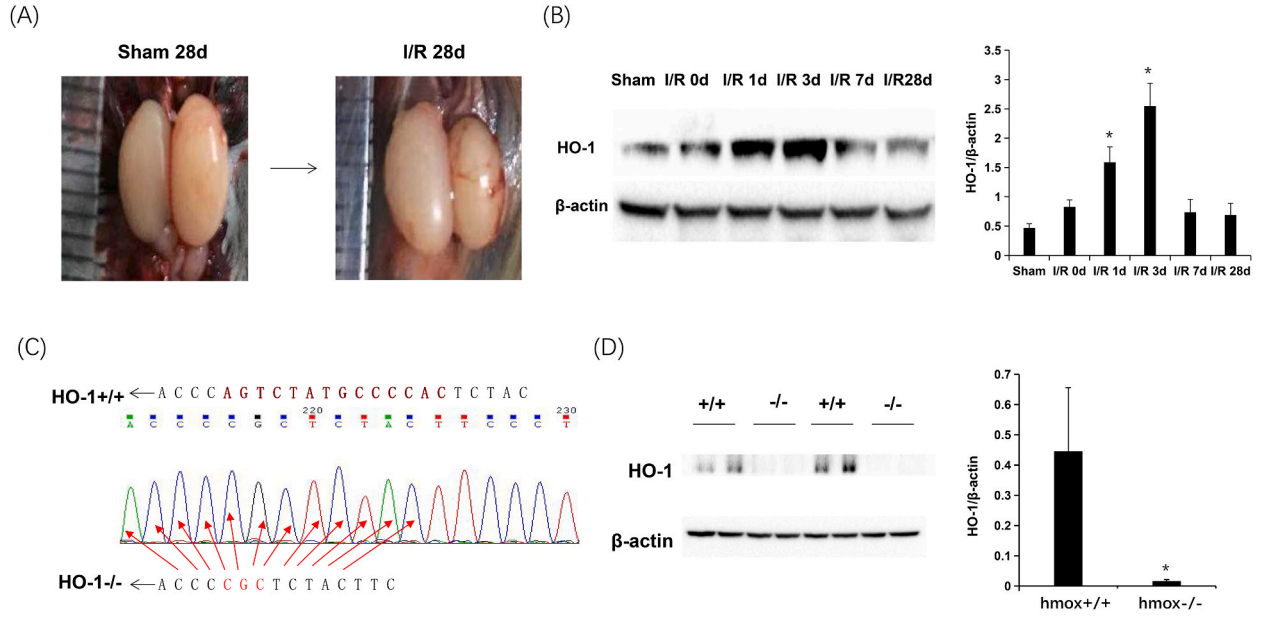

Fig. 1. HO-1 plays a role in the response to testicular I/R injury. (A) Representative testes from rats (day 28) demonstrating differences in size between the sham (the left testis were positioned through a left scrotal incision without torsion for 28 days) and I/R (the left testis was subjected to torsion for 2 h, and was allowed to return to their natural position for 28 days) groups. (B) Protein expression and densitometric analysis of HO-1 were analysed at the indicated time points by western blotting after testicular I/R (n = 3, the original image is provided in the Supplementary Fig. 1). *p < 0.05 compared with the sham group. (C) Sequencing chromatograms show the 11 bp deletion before CACTCTACTT, and the mutation before CTCTACTTC of the two strands is A to G in the homozygous rat ($hmox^{-/-}$) testis sample. (D) Representative western blots and densitometric analysis showing HO-1 expression in WT and $hmox^{-/-}$ rats under basal conditions (n = 4, the original image is provided in the Supplementary Fig. 2).*p < 0.05 compared with the $hmox^{+/+}$ group. HO-1, heme oxygenase-1; I/R, ischaemia/injury; WT, wild-type.

2.5. Histopathologic examination

After neutral fixation with 10 % formalin, testicles were embedded in paraffin wax and sectioned for histopathological examination. After xylene dewaxing, ethanol dehydration, and haematoxylin and eosin (H&E) staining, images were obtained and viewed under an inverted microscope (Nikon TE 2000-U, Japan); Johnsen's score [14] was determined by two pathologists blinded to the experiment.

2.6. Immunofluorescence and immunohistochemistry

Briefly, GC-1 cells were fixed with 4 % paraformaldehyde and washed. The cells were permeabilised with 0.1 % Triton X-100, incubated overnight with an anti–HO–1 antibody (1:200; Cell Signalling Technology, Danvers, MA, USA), and incubated with anti-goat IgG for 1 h (diluted 1:800; Cell Signalling Technology). Subsequently, cells were subjected to DAPI staining (1:2000). Finally, the slides were analysed under an inverted microscope and fixed in 4 % paraformaldehyde for immunohistochemical analysis. After sectioning, dewaxing, and hydration, the antigens were extracted by microwaving. Anti–HO–1 antibody (1:200; Cell Signalling, Danvers, MA) was added and incubated for 2 h. Horseradish (HRP)-labelled antibody 2 was incubated at 37 °C for 1 h. All samples were stained with DAPI (KeyGEN BioTECH, Nanjing, China) and viewed under a fluorescence microscope.

2.7. Biochemical marker assay

Levels of serum testosterone and FSH were detected by radioimmunoassay (RIA) with kits purchased from Jiuding Medical Bioengineering Co., Ltd (Tianjin).

2.8. Western blotting

Proteins were extracted from the testicular tissue using a lysis buffer. After sodium dodecyl sulfate-polyacrylamide gel electrophoresis, the proteins were transferred onto a nitrocellulose film. After blocking, the membrane was treated with primary anti–HO–1 antibody (1:500; Cell Signalling, Danvers, MA, USA), p-*c*-Jun (1:1000; Abcam, Cambridge, MA, USA), c-Jun (Abcam), tubulin (1:1000; Abcam), and-actin (1:1000; Abcam). The membrane was thoroughly cleansed, incubated with an HRP-conjugated antibody, and detected using an ECL kit (Pierce Biotechnology, Rockford, USA).

2.9. Determination of HO enzymatic activity

As previously described, HO activity was measured by detecting the amount of cell lysate-generated CO [15].

2.10. Construction of HO-1 eukaryotic overexpression vector

HO-1 eukaryotic overexpression vectors were obtained from Guangzhou Ruibo Biotechnology Co., Ltd, as described previously [15]. Mutant HO-1 (△hHO-1) GC-1 cells exhibited similar protein expression to wild-type (WT) hHO-1 (wtHO-1); however, HO activity was markedly lower than that of wtHO-1.

2.11. Assessment of apoptosis and cell cycle analysis

At the end of incubation, cells were collected using 0.05 % trypsin-EDTA, immunostained with Annexin V-FITC (5 μg/mL; BD Biosciences, Franklin Lakes, USA) in a buffer medium, and analysed by flow cytometry (Becton, Dickinson and Company, BD, NJ, USA). For cell cycle analysis, cells were fixed with 70 % ethanol at the end of the incubation period, stained with propidium iodide (PI), and analysed by flow cytometry.

2.12. High-resolution mRNA sequencing and data processing

Total RNA was isolated using TRIzol reagent (Invitrogen, Carlsbad, CA, USA) according to the manufacturer's instructions. Sera-Mag magnetic oligo (dT) beads (Sigma-Aldrich, St. Louis, MO, USA) were used to isolate 10 μg of total poly(A) mRNA and establish a paired RNA-seq library for transcription analysis. A fragment of appropriate size was selected and enlarged using PCR. The paired RNA-SEQ ™ libraries (PE) were prepared and sequenced using the Illumina HiSeq 2500 platform according to the manufacturer's protocol. High-throughput sequencing was performed by Beijing Orysson Technology Co., Ltd. (Beijing, China). The results of the differential gene expression (DE) were obtained using DEGseq2, based on the change in yield level ($p < 0.05$, FC > 2). Kyoto Encyclopedia of Genes and Genomes (KEGG) pathway annotation was performed using the BLASTall software instead of the KEGG database. The RNA-Seq data has been assigned GEO accession number GSE237565.

2.13. High-resolution miRNA sequencing and data processing

Total RNA was extracted from the testicles using TRIzol (Ambion, Austin, Texas, USA), and RNA integrity was measured using an

Agilent 2100 (Agilent Technologies, Palo Alto, USA). Using the TruSeq™ Small RNA Sample preparation kit (Illumina, San Diego, California), a small RNA library was acquired from 1 g of total RNA. Briefly, RNA to which the adapter was connected was reverse-transcribed using Superscript III (Invitrogen, Carlsbad, California, USA), and PCR amplification was performed with the synthesised cDNA as the template. Amplified DNA was isolated from polyacrylamide gels. A portion corresponding to the size range of a small RNA molecule connected to an adapter was separated from the gel. The yields of small RNA libraries were measured using KAPA Biosystems qRT-PCR kits. An insertion control group was created using the Phix Control Kit (Illumina, San Diego, California, USA). A 50–51 nt single-platform entry was performed on the Illumina MiSeq and Illumina 1500 platforms.

2.14. RT-qPCR

Total RNA was harvested from the testis tissue using TRIzol reagent (Thermo Fisher Technologies, Waltham, USA). PCR was performed using a TaqMan instrument and an SYBR quantitative Green PCR kit (Takara Bio, Japan). Gene expression levels were quantified using a PCR Rapid Real-Time 7500 device according to the manufacturer's instructions. The reactor was rolled in 384 good plates for 30 s at 95 °C bottom half, 40 cycles at 95 °C for 5 s, and then 30 s at 60 °C bottom half. The CT value was calculated and compared for relative quantification. Table 1 lists the primers used for RT-qPCR.

2.15. Plasmids, siRNAs, and transfection

The PCMV6-empty plasmid vector (Origene Technologies, MD, USA) and PCMV6 c-Jun cDNA (Gene ID: 16,476) were manufactured using clonal reagent kits (Vzayme, Nanjing, China). Knockdown experiments were performed using HO-1 and c-Jun siRNA sequences (RiboBio, Guangzhou, China). For short transgenic plasmids or siRNA, GC-1 cells were cultured in complete growth culture medium until fusion reached 70 %. The cells were then transfected with Lipofectamine 2000 in serum-free RPMI-1640 medium. After 12 h, the incubator was converted to a full-growth incubator, and incubation was performed for 24 h.

2.16. Plasmid construction and luciferase reporter assays

The estimated and mutated miR221/222 target binding sequences were synthesised from C-Jun and cloned into a luciferase reporter plasmid to generate a WT C-Jun (C-Jun -WT) or mutant C-jun (C-jun-mut) reporter plasmid. C-jun 3′UTR mutant sequences were obtained by overlap expansion PCR, and WT and mutant sequences were cloned into the psiCHECK-2 vector (Promega, Madison, WI, USA). For luciferase reporter assay, GC-1 cells were plated in 24-well plates. Cells were then co-transfected with the imitation miR221/222 or the negative control group miR221/222 using Lipofectamine 2000 (Invitrogen, USA). Forty-eight hours after infection, luciferase was detected using a dual-luciferase reporter detection system (Promega, Madison, WI, USA).

2.17. Statistical analysis

Data are presented as the mean ± standard deviation (SD) of at least three independent experiments. The statistical analysis was performed using one way analysis of variance (ANOVA) followed by Dunnett's T3 for multiple comparisons. Differences were considered statistically significant at $p < 0.05$.

Table 1
List of primers used for qRT-PCR.

Gene	Foward primer (5'-> 3')
miR221–3p	AGCUACAUUGUCUGCUGGGUUUC
miR222–3p	AGCUACAUCUGGCUACUGGGU
miR125b-2-3p	ACAAGUCAGGUUCUUGGGACCU
miR200a-5p	CAUCUUACCGGACAGUGCUGGA
miR429	UAAUACUGUCUGGUAAUGCCGU
ATP8A2	CAGTGGGAGACATCGTGAAGG
FAM196B	CCTGTGCTCCTAAAGCGAAG
SLC4A4	GATGCCACCGACAACATGC
FNIP2	CATTTAGCTTGGCCGAAGAAAC
TOX	GCTCCCGTTCCATCCACAAA
HO-1	AAGCCGAGAATGCTGAGTTCA
c-jun	AGCATGACCCTGAACCTGG

Abbreviations:ATP8A2, ATPase phospholipid transporting 8A2; FAM196B, family with sequence similarity 196, member B; SLC4A4, solute carrier family 4 member 4; FNIP2, folliculin Interacting protein 2; TOX, thymocyte selection associated high mobility group box; HO-1: heme oxygenase.

3. Results

3.1. HO-1 plays a role in testicular I/R injury

We compared testes weights between the I/R and sham groups and found that the testes of the I/R group were smaller than those of the sham group on day 28 (Fig. 1A). To explore the function of HO-1 in testicular I/R injury, we examined whether I/R injury could induce HO-1 expression. The level of HO-1 gradually increased following testicular I/R injury, peaking on day 3 and recovering on days 7 and 28, thereby suggesting the possible involvement of HO-1 in testicular I/R injury (Fig. 1B). Therefore, we established global HO-1 knockout rats (Fig. 1C and D). Under basal conditions, HO-1−/− rats grew normally and appeared healthy, with testicular structure and morphology similar to those of control rats (Fig. 2C).

3.2. Effect of HO-1 on testicular I/R injury in vivo

Plasma testosterone levels gradually decreased after testicular I/R injury, with a remarkable change detected on day 1 (both $hmox^{+/+}$ and $hmox^{-/-}$ groups) and day 3 ($hmox^{+/+}$ group) when compared with levels in the sham group; testosterone levels recovered on days 7 and 28 and they were significantly reduced in $hmox^{-/-}$ groups when compared with those in WT groups (Fig. 2A). Conversely, plasma FSH levels gradually increased after testicular I/R injury, with significant alterations observed on days 1 and 3 (both $hmox^{+/+}$ and $hmox^{-/-}$ groups) when compared with those in the sham group; the levels recovered on days 7 and 28 and were significantly increased in $hmox^{-/-}$ groups when compared with those in WT groups (Fig. 2B).

Using H&E staining, we examined testicular tissue samples of sham rats and those of rats subjected to 2 h of ischaemia, followed by 0, 1, and 3 days of reperfusion, respectively. Pathophysiological changes indicated the successful establishment of the testicular I/R injury model. Compared with the sham group, the testis of the $hmox^{-/-}$ group exhibited ischaemia, with notable injury-induced changes and a reduced score. Compared with the sham group, $hmox^{+/+}$ and $hmox^{-/-}$ groups subjected to reperfusion for 1 and 3 days following ischaemia showed severe injury (including irregular and atrophic seminiferous tubules morphology and germinal cell sloughing) and a significantly reduced score. $Hmox^{-/-}$ rats grew normally and appeared healthy, with a similar testicular structure and morphology to WT rats. However, the $hmox^{-/-}$ rats testis showed ischaemia only or I/R-induced notable injury, along with

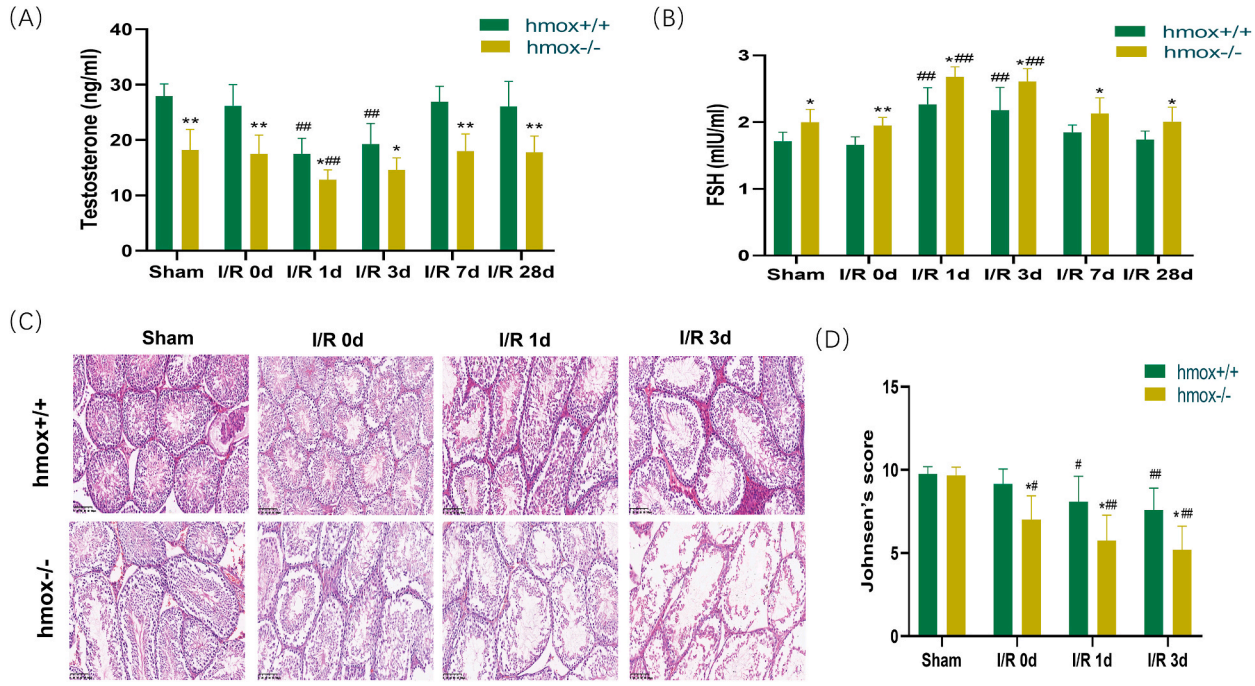

Fig. 2. Effect of HO-1 on testicular I/R injury *in vivo*. (A) Serum testosterone and (B) FSH levels were evaluated by enzyme-linked immunosorbent assay in sham and I/R groups on 0, 1, 3, 7, and 28 days (n = 5). I/R injury reduces testosterone levels, and HO-1 gene knockout exacerbates this trend. The trend of FSH levels is opposite.*p < 0.05, **p < 0.01 compared with the $hmox^{+/+}$ group in sham or the indicated time points I/R groups, respectively; #p < 0.05, ##p < 0.01 compared with the sham group in $hmox^{+/+}$ group or $hmox^{-/-}$ group, respectively. (C) Representative microscopic findings of rats testicular tissue in sham and I/R groups on 0, 1, and 3 days. Tissue sections were stained with haematoxylin-eosin. Scale bar = 100 μm. (D) Johnsen's score was determined for each group at each time point after the sham operation or I/R (n = 5). I/R injury decreased the Johnsen's scores, and HO-1 gene knockout further decreased the scores.*p < 0.05 compared with the $hmox^{+/+}$ group in sham or the indicated time points I/R groups, respectively; #p < 0 05, ##p < 0.01 compared with the sham group in $hmox^{+/+}$ group or $hmox^{-/-}$ group, respectively. FSH, follicle-stimulating hormone; HO-1, heme oxygenase-1; I/R, ischaemia/injury.

reduced scores, compared with those of hmox$^{+/+}$ rats (Fig. 2C and D).

3.3. Nuclear translocation of HO-1 in GC-1 cells

Based on our H&E staining results, nuclear translocation of HO-1 occurred during I/R injury, with deposition on the basement membrane of the seminiferous tubules *in vivo*, thereby suggesting that spermatogonial stem cells (SSCs) probably play an important role in testicular I/R injury (Fig. 3A); these observations were next confirmed *in vitro*. We used GC-1, GC-2, TM3, and TM4 cells to simulate testicular SSCs and spermatocyte, Leydig, and Sertoli cells, respectively. In GC-1 cells, fluorescence localisation of HO-1 in the H/R, WtHO-1, △hHO-1, and empty vector control group revealed that H/R, WtHO-1, and △hHO-1 induced the nuclear translocation of HO-1, and H/R injury increased the HO-1 level in GC-1 cells (Fig. 3B–D). However, the same trend was not observed in other cell lines (Fig. 3C and D).

3.4. Effect of HO-1 nuclear translocation on GC-1 cell cycle and death

The nuclear translocation of HO-1 could decrease HO activity, and leptomycin B (LMB, an inhibitor of extranuclear transport, verified in this experiment as an inhibitor of inward transport) suppressed HO-1 nuclear transport to restore HO activity. The HO activity of the △HO-1 group was significantly lower than that of the WtHO-1 group (Fig. 4A). Silencing HO-1 and overexpression of △hHO-1 could significantly enhance and ameliorate testicular injury, respectively. Silencing of HO-1 increased apoptosis, whereas hHO-1 overexpression had the opposite effect (Fig. 4B). Compared with the normal control (NC) group, GC-1 cells in the S-phase were reduced in the H/R group, with a concomitant elevation in cells in the G0/G1 phase. Compared with the H/R-only group, silencing HO-1 in the H/R group decreased GC-1 cells in S-phase, with a concomitant increase in G0/G1 phase; however, the opposite effect was observed on overexpression of △hHO-1. Combined with the apoptosis results, we speculated that the increased percentage of GC-1 cells in the S phase could be attributed to enhanced GC-1 cell proliferation (Fig. 4C).

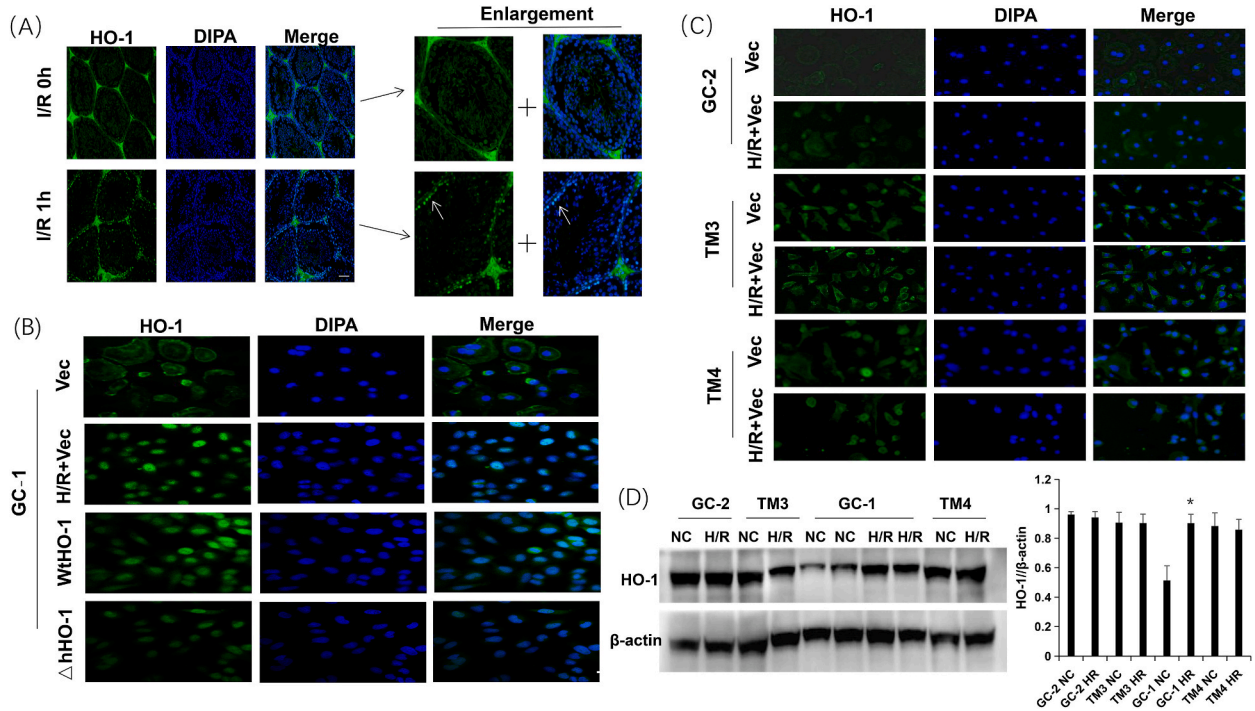

Fig. 3. Nuclear translocation of HO-1. (A) Fluorescence nuclear translocation of HO-1 was observed *in vivo* in the I/R 1h group compared to the control group (I/R 0h). Local magnification is shown on the right side of the image, with the white arrow indicating SSCs. (B) In GC-1 cells, the fluorescence nuclear translocation of HO-1 can be observed in H/R, WtHO-1, and △hHO-1 groups, compared to the empty vector control groups. (C) In GC-2, TM3, and TM4 cells, fluorescence nuclear translocation of HO-1 can't be observed in the H/R and empty vector control groups. Bar = 100 μm. (D) Representative western blots and densitometric analysis showing HO-1 expression in control and H/R groups of GC-1, GC-2, TM3, and TM4 cells (the original image is provided in the Supplementary Fig. 3). H/R increased the expression level of HO-1 in GC-1 cells, but this was not found in other cells. *p < 0.05 compared with the NC group. HO-1, heme oxygenase-1; I/R, ischaemia/injury.

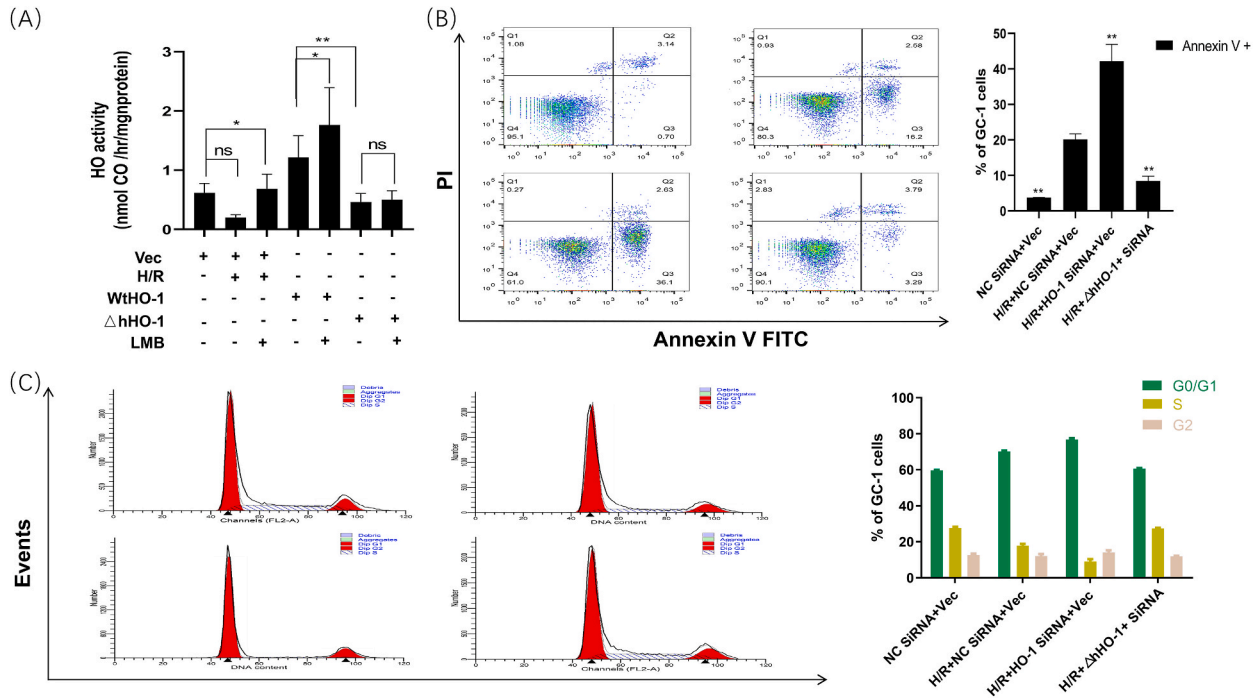

Fig. 4. Effect of HO-1 nuclear importation on GC-1 cell cycle and death. (A) HO activity detection in empty vector control, H/R, WtHO-1, △hHO-1, and LMB groups. T. The △HO-1 group exhibited significantly lower HO activity than the WtHO-1 group, and △hHO-1 induced the nuclear translocation of HO-1.(B) Cells were stained with propidium iodide (PI) and analysed by flow cytometry. The columns represent the percentage of both early and late apoptotic cells. Silencing HO-1 and overexpression of △hHO-1 could significantly enhance and ameliorate cell apoptosis. **p < 0.01 versus the H/R + NC SiRNA + Vec group. (C) Cells were incubated with Annexin V-FITC and PI and analysed by flow cytometry. The columns represent the percentage of different phases of the cell cycle. Silencing HO-1 and overexpression of △hHO-1 could significantly decrease and enhance cell proliferation. **p < 0.01 and ##p < 0.01 versus the H/R + NC SiRNA + Vec group at G0/G1 and S phases, respectively. HO-1, heme oxygenase-1; H/R, hypoxia/reperfusion; LMB, Leptomycin B (an inhibitor of extranuclear transport, verified in this experiment as an inhibitor of inward transport).

3.5. Gene sequencing analysis of testicular I/R injury-related genes with strong conservation in HO-1 knockout rats: miR221/222 and its downstream gene TOX

Gene sequencing was performed to detect changes in miRNA and mRNA expression profiles in testicular tissues after HO-1 knockout (Fig. 5A and 6A). Using bioinformatics analysis and the accumulated literature, we screened for miR-221–3p, miR-222–3p, miR125b-2-3p, miR200a-5p, miR429, ATPBA2, TOX,FAM196B,SLC4A4, and FNIP2 with high diversity and strong conservation. Changes in expression were measured at the molecular level. We observed that miR221/222 was strongly conserved, with the most significant DE; screening identified the downstream gene TOX (Fig. 5B and 6B,C).

3.6. HO-1 activates c-Jun to impact miR-221/222 transcription

Western blotting was performed to confirm the interaction between HO-1 and p-*c*-Jun. Compared with NC group cells, H/R increased HO-1 levels in GC-1 cells, while silencing HO-1 in the H/R group decreased c-Jun phosphorylation; however, overexpression of HO-1 had the opposite effect (Fig. 7A). RT-qPCR was performed to confirm potential regulatory relationships between HO-1, c-Jun, and miR-221/222. We knocked down c-Jun in GC-1 cells and observed a decrease in miR-221/222 expression. Inhibition of HO-1 expression reduced the expression of c-Jun and miR-221/222, which was rescued by adding c-Jun (Fig. 7B). Moreover, the dual-luciferase reporter assay confirmed the interaction between c-Jun and miR-221/222 (Fig. 7C).

4. Discussion

To the best of our knowledge, for such instances, there may be other studies happening elsewhere in the world in this regard, or similar studies may be in the process of publication, or even already published in other languages. We, for the first time, identified that HO-1 could activate the phosphorylation of c-Jun in the nucleus and bind to phosphorylated c-Jun. In addition, binding of c-Jun to the promoter region of miR-221/222 activated miR-221/222, whereas binding of miR-221/222 to the 3' UTR of its target gene TOX leads to TOX degradation and/or translation inhibition. These findings suggested that induction of the phosphorylated-*c*-Jun-miR-221/222-

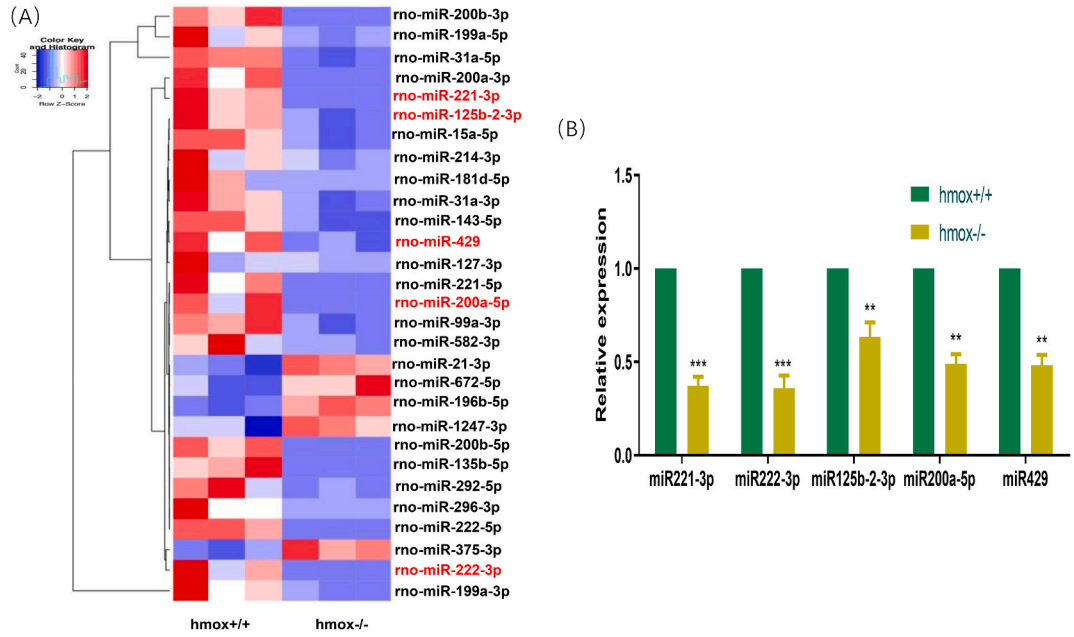

Fig. 5. Gene sequencing analysis of HO-1 knockout rats testis for I/R injury-related miRNAs with strong conservation. (A) Hierarchical clustering of the transcriptome showing the different miRNAs expression profiles in HO-1 knockout versus wild-type (WT) rats testis with I/R injury. The color key on the top-left side of the figure indicates expression levels. (B) RT-qPCR was used to verify miRNAs with large difference.**$p < 0.01$ and ***$p < 0.001$ versus the $hmox^{+/+}$ group. HO-1, heme oxygenase-1; I/R, ischaemia/injury; RT-qPCR, reverse transcription-quantitative PCR. (For interpretation of the references to color in this figure legend, the reader is referred to the Web version of this article.)

TOX pathway by HO-1 is an adaptive mechanism during testicular I/R injury and that induction of the HO-1-phosphorylated-*c*-Jun-miR-221/222-TOX axis expression may be a new therapeutic target for testicular I/R injury. Fig. 8 illustrates potential mechanisms related to HO-1 function contributing to GC-1 protection following H/R injury.

First, we demonstrated that the effects of early I/R injury on the rats testes were not transient. We compared the testis weights between the I/R and sham groups, revealing that the testes of the I/R group were smaller than those of the sham group on day 28. HO-1 has been found to play a role in maintaining cellular homeostasis and is critical for protecting different organs and tissues from I/R injury by reducing oxidative damage, inhibiting apoptosis, and attenuating inflammatory responses; however, the underlying mechanism remains unclear. *Smilax excelsa* L. was shown to prevent tissue damage in a murine torsion model by exerting antioxidant and anti-inflammatory effects and activating the Nrf-2/HO-1 pathway [16]. Consistently, the level of HO-1 gradually increased after testicular I/R injury, reached the highest level on day 3, and recovered on days 7 and 28, thereby suggesting possible involvement of HO-1 in the process of testicular I/R injury. Next, we measured testosterone and FSH levels and pathological changes at different time points after HO-1 knockout. Testosterone triggers spermatogenesis in combination with FSH. The joint action of testosterone and FSH is exerted on Sertoli cells, supporting the gradual development of germ cells into mature sperm [17]. Herein, plasma testosterone gradually decreased after testicular I/R injury when compared with that in the sham group; the level recovered on days 7 and 28. Moreover, the plasma testosterone level was significantly reduced in the $hmox^{-/-}$ group when compared with that in the WT group. Conversely, the plasma FSH level gradually increased after testicular I/R injury when compared with that in the sham group, recovering on days 7 and 28. Compared with the WT group, the $hmox^{-/-}$ group showed a significant increase in the plasma FSH level. As previously described [18,19], we used H&E and Johnsen's score to evaluate pathophysiological injuries, for example, severe pathophysiological injuries including irregular and atrophic seminiferous tubules morphology, as well as germinal cell sloughing corresponds to a low Johnsen's score. Groups subjected to reperfusion for 1 and 3 days, respectively, after ischaemia showed severe pathophysiological injuries with a significant reduction in the Johnsen's scores in both $hmox^{+/+}$ and $hmox^{-/-}$ groups when compared with the sham group. Compared with the $hmox^{+/+}$ groups, the testis of the $hmox^{-/-}$ groups experienced ischaemia only or exhibited marked injury and a reduced score following I/R injury. These findings suggest that HO-1 plays an important role in testicular I/R.

Next, we investigated the cells that play a major role in HO-1 activity against testicular I/R injury. It has been reported that the application of etomidate prior to testicular detorsion could largely suppress germ cell damage and Leydig cell loss in the ipsilateral tissue, indicating that Leydig cells may play an important role in testicular I/R injury [20]. Ferroptosis has been associated with oxygen-glucose deprivation/reoxygenation-induced Sertoli cell death, further revealing the key role of Leydig cells in testicular I/R injury [21]. Interestingly, our H&E staining results revealed that the I/R injury could induce nuclear translocation of HO-1, which was deposited on the basement membrane of the seminiferous tubules *in vivo*; this finding suggested that SSCs probably play an important role in testicular I/R injury. We then confirmed it in GC-1 cells *in vitro*. These results indicated that HO-1 probably acts via SSCs in testicular I/R injury.

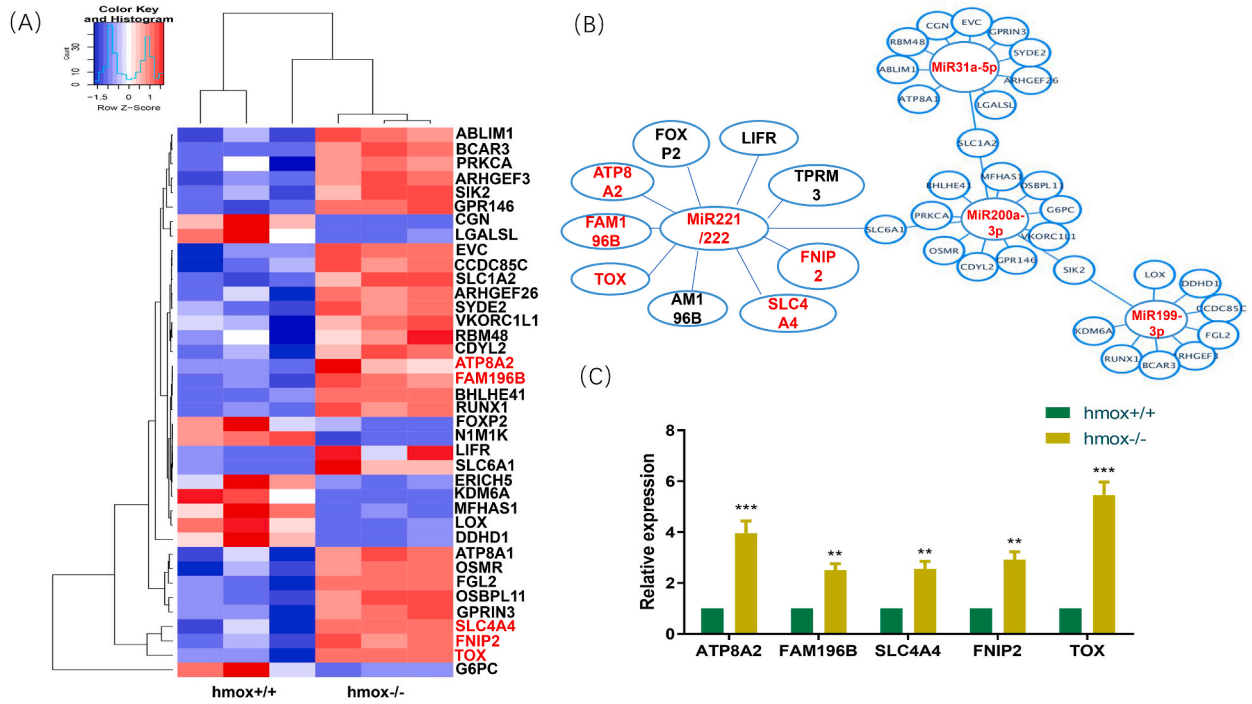

Fig. 6. The section of miR221/222 and its downstream gene based on gene sequencing and bioinformatics analysis. (A) mRNA expression profile of rats I/R testis tissue after HO-1 knockout was detected by gene sequencing. The color key on the top-left side of the figure indicates expression levels. (B) Gene co-expression network diagram. (C) Combined with miRNA results, the selected miR221/222 shows strong conservation with the most significant differential expression, with its downstream genes verified by qRT-PCR.**$p < 0.01$ and ***$p < 0.001$ versus the $hmox^{+/+}$ group. HO-1, heme oxygenase-1; I/R, ischaemia/injury; RT-qPCR, reverse transcription-quantitative PCR. (For interpretation of the references to color in this figure legend, the reader is referred to the Web version of this article.)

HO-1 is a commonly expressed, inducible enzyme that degrades heme into CO, bilirubin, and Fe^{2+} [5]. However, it is yet to be established whether HO-1 protein itself or heme breakdown metabolites play a role in cell signalling. Accordingly, we used △HO-1 to confirm the role of HO-1. The △HO-1 group exhibited significantly lower HO activity than the WtHO-1 group, and △hHO-1 induced the nuclear translocation of HO-1, as observed in WtHO-1 GC-1 cells. Silencing HO-1 and overexpression of hHO-1 could significantly enhance and ameliorate testicular injury, respectively, indicating that the HO-1 protein itself, rather than the heme breakdown metabolites, might play a key role in testicular I/R injury.

Next, we preliminarily explored the specific mechanism of HO-1 in testicular I/R injury. Most studies on HO-1 have failed to explore underlying mechanisms, with limited data on potential mechanisms reported by Kojiro et al. HO-1 was shown to regulate macrophage activation and hepatocyte death in hepatic I/R injury through the sirtuin1-p53 signalling network [8]. HO-1 knockdown upregulated the expression of vascular cell adhesion molecule 1 to induce neutrophil recruitment during renal I/R injury [22]. However, the above experiments did not explore whether HO-1 can impact its own activity or whether heme metabolites influence its activity; in particular, limited data are available on the role of HO-1 in testicular I/R injury. Thus, we performed gene sequencing to detect changes in miRNA and mRNA expression profiles in testicular tissues derived from HO-1 knockout rats. Based on bioinformatics analysis and available literature, we screened out miR-221–3p, miR-222–3p, miR125b-2-3p, miR200a-5p, miR429, ATPBA2, TOX, FAM196B, SLC4A4, and FNIP2 with high diversity and strong conservation. miR221/222 was strongly conserved, exhibiting the most significant DE; we identified the downstream gene TOX on screening.

Growing evidence suggests that miRNAs play a role in I/R injury [10,11]. c-Jun has been associated with the activation of miR-221/222 in prostate cancer and glioblastoma [12]. Combined with the above theoretical basis, we speculated whether HO-1 could activate miR-221/222 by interacting with phosphorylated c-Jun in testicular I/R injury. The interaction between HO-1 and phosphorylated c-Jun was preliminarily confirmed by western blotting; silencing HO-1 in the H/R group decreased the phosphorylation of c-Jun, whereas overexpression of HO-1 had the opposite effect, and the possible regulatory relationship of HO-1, c-Jun, or miR-221/222 was verified by RT-qPCR. Consistent with the HO-1 inhibition results, a dual-luciferase reporter assay confirmed the interaction between c-Jun and miR-221/222. These results indicate that the HO-1-phosphorylated c-Jun-miR-221/222-TOX axis may be crucial in testicular I/R injury.

5. Limitations of the study

The present study had several limitations. Herein, we failed to overexpress HO-1 *in vivo*. Given that testis has a blood-testis barrier,

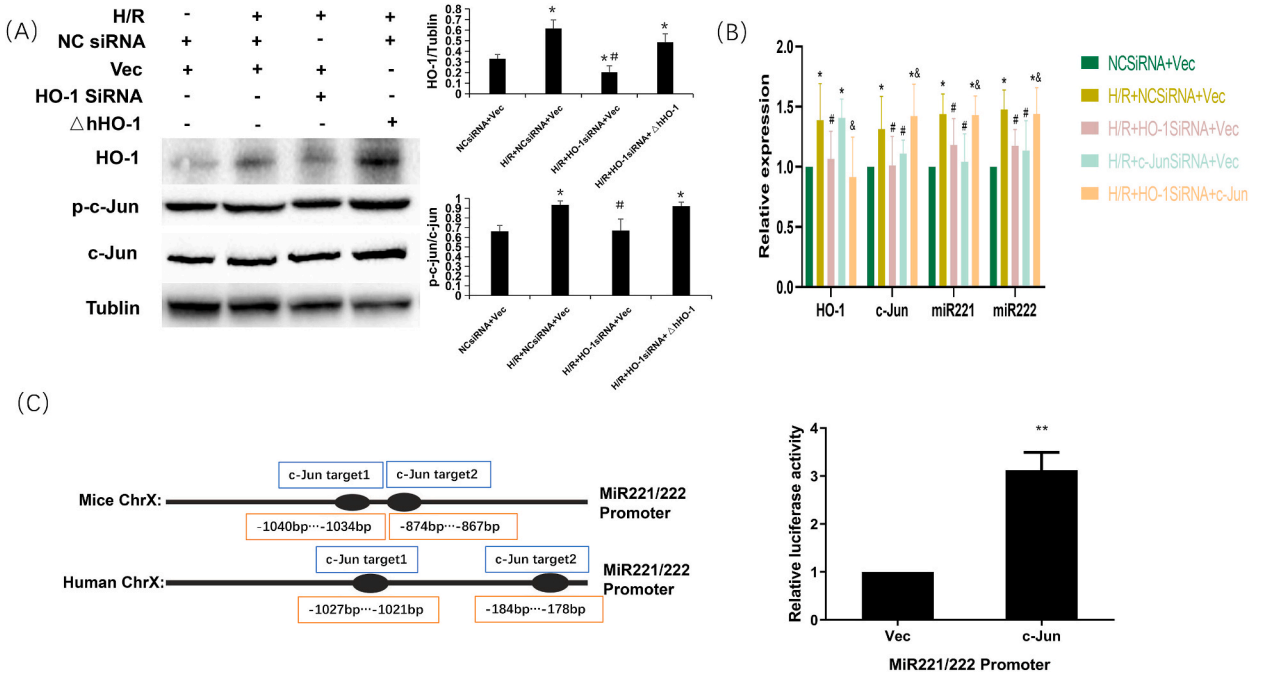

Fig. 7. HO-1 activates c-Jun to affect miR-221/222 transcription. (A) Representative western blots and densitometric analysis showing HO-1 activates c-Jun (the original image is provided in the Supplementary Fig. 4). (B) The possible regulatory relationship between HO-1, c-Jun, and miR-221/222 was verified using RT-qPCR. HO-1 activates c-Jun to affect miR-221/222.*$p < 0.05$ versus the NC siRNA + Vec group, #$p < 0.05$ versus the H/R + NC siRNA + Vec group, and &$p < 0.05$ versus the H/R+ c-Jun siRNA + Vec group. (C) Dual-luciferase reporter assay was performed to confirm the interaction between c-Jun and miR-221/222. **$p < 0.01$ versus Vec group. HO-1, heme oxygenase-1; I/R, ischaemia/injury; LMB, Leptomycin B; RT-qPCR, reverse transcription-quantitative PCR.

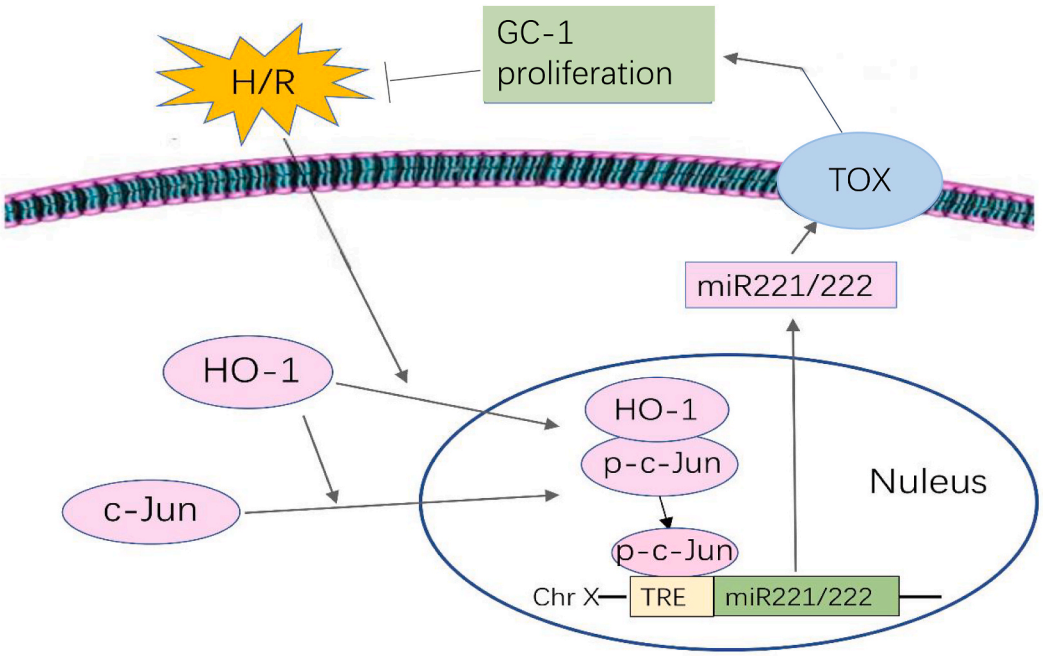

Fig. 8. Summary diagram illustrating the possible mechanisms associated with HO-1 function and contributing to GC-1 protection following hypoxia/reperfusion (H/R) injury.

intraperitoneal injection and other methods are often ineffective; hence, we attempted microinjection of reticulum testis and injected adenovirus packaged with an expression vector, but were unsuccessful. We are updating the injection protocol and method and believe our unremitting efforts will be successful. Our research on the mechanism of the HO-1-phosphorylated c-Jun-miR-221/222-TOX axis is preliminary, and additional experiments are needed to further verify the relationship between them *in vitro* and *in vivo*. Interestingly, HO-1 expression increased during the early stage of I/R injury, which was hypothesised to be a stress-protective response of the body to damage. Based on the changes in testosterone levels in testicular I/R and HO-1 knockout rats, we initially assumed the primary involvement of testicular interstitial cells. However, given that the results suggest that HO-1 expression was unaltered *in vitro* and *in vivo*, we suspect a role of heme breakdown. Additional studies are required to corroborate these hypotheses. These seemingly contradictory or interesting experimental results confirm that the local testicular microenvironment is markedly complex. There are currently no commercial rat spermatogonial, Sertoli cell lines, etc., so we used commercial mouse cell lines to instead of them. And The results may vary due to species differences. In the future, we hope to successfully isolate primary cells to verify our results.

6. Conclusion

Our results suggest that HO-1 might attenuate testicular I/R injury by activating the phosphorylated c-Jun-miR-221/222-TOX pathway. Therefore, pharmacological targeting of the HO-1-phosphorylated c-Jun-miR-221/222-TOX axis may have potential implications in clinical practice.

Data availability statement

The gene sequencing analysis of testicular I/R injury-related genes in HO-1 knockout rats had been deposited into GEO database (GSE237565).

CRediT authorship contribution statement

Bo Xie: Project administration. **Bing Cheng:** Writing – original draft. **Lugeng He:** Software, Data curation. **Yunfu Liu:** Writing – review & editing. **Ning He:** Validation, Methodology.

Declaration of competing interest

The authors declare that they have no known competing financial interests or personal relationships that could have appeared to influence the work reported in this paper.

Acknowledgements

Not applicable.

Appendix A. Supplementary data

Supplementary data to this article can be found online at https://doi.org/10.1016/j.heliyon.2024.e24579.

References

[1] H. Thaker, C.P. Nelson, Adjuvant pharmacological and surgical therapy for testicular torsion: current state of the art, J. Pediatr. Urol. 16 (6) (2020) 807–814, https://doi.org/10.1016/j.jpurol.2020.08.005.
[2] A. Raisi, A. Kheradmand, G. Farjanikish, F. Davoodi, S. Taheri, Nitroglycerin ameliorates sperm parameters, oxidative stress and testicular injury following by testicular torsion/detorsion in male rats, Exp. Mol. Pathol. 117 (2020) 104563, https://doi.org/10.1016/j.yexmp.2020.104563.
[3] S. Vasconcelos-Castro, B. Flor-de-Lima, J.M. Campos, M. Soares-Oliveira, Manual detorsion in testicular torsion: 5 years of experience at a single center, J. Pediatr. Surg. 55 (12) (2020) 2728–2731, https://doi.org/10.1016/j.jpedsurg.2020.02.026.
[4] C. Ho, R.S. Zee, N. Omidi, C. Bayne, A. Hester, E. Mukherjee, et al., Varenicline limits ischemia reperfusion injury following testicular torsion in mice, J. Pediatr. Urol. 17 (5) (2021) 631, https://doi.org/10.1016/j.jpurol.2021.07.004, e1-.e8.
[5] N. He, J.J. Jia, H.Y. Xie, J.H. Li, Y. He, S.Y. Yin, et al., Partial inhibition of HO-1 attenuates HMP-induced hepatic regeneration against liver injury in rats, Oxid. Med. Cell. Longev. 2018 (2018) 9108483, https://doi.org/10.1155/2018/9108483.
[6] H. Dong, Z. Qiang, D. Chai, J. Peng, Y. Xia, R. Hu, et al., Nrf2 inhibits ferroptosis and protects against acute lung injury due to intestinal ischemia reperfusion via regulating SLC7A11 and HO-1, Aging 12 (13) (2020) 12943–12959, https://doi.org/10.18632/aging.103378.
[7] Z. Lv, F. Wang, X. Zhang, X. Zhang, J. Zhang, R. Liu, Etomidate attenuates the ferroptosis in myocardial ischemia/reperfusion rat model via Nrf2/HO-1 pathway, Shock 56 (3) (2021) 440–449, https://doi.org/10.1097/shk.0000000000001751.
[8] K. Nakamura, M. Zhang, S. Kageyama, B. Ke, T. Fujii, R.A. Sosa, et al., Macrophage heme oxygenase-1-SIRT1-p53 axis regulates sterile inflammation in liver ischemia-reperfusion injury, J. Hepatol. 67 (6) (2017) 1232–1242, https://doi.org/10.1016/j.jhep.2017.08.010.
[9] M. Rossi, K. Korpak, A. Doerfler, K. Zouaoui Boudjeltia, Deciphering the role of heme oxygenase-1 (HO-1) expressing macrophages in renal ischemia-reperfusion injury, Biomedicines 9 (3) (2021), https://doi.org/10.3390/biomedicines9030306.
[10] L. Yuan, W. Chen, J. Xiang, Q. Deng, Y. Hu, J. Li, Advances of circRNA-miRNA-mRNA regulatory network in cerebral ischemia/reperfusion injury, Exp. Cell Res. 419 (2) (2022) 113302, https://doi.org/10.1016/j.yexcr.2022.113302.

[11] E. Jayawardena, L. Medzikovic, G. Ruffenach, M. Eghbali, Role of miRNA-1 and miRNA-21 in acute myocardial ischemia-reperfusion injury and their potential as therapeutic strategy, Int. J. Mol. Sci. 23 (3) (2022), https://doi.org/10.3390/ijms23031512.
[12] S. Galardi, N. Mercatelli, M.G. Farace, S.A. Ciafrè, NF-kB and c-Jun induce the expression of the oncogenic miR-221 and miR-222 in prostate carcinoma and glioblastoma cells, Nucleic Acids Res. 39 (9) (2011) 3892–3902, https://doi.org/10.1093/nar/gkr006.
[13] Z. Qin, K. Zhu, J. Xue, P. Cao, L. Xu, Z. Xu, et al., Zinc-induced protective effect for testicular ischemia-reperfusion injury by promoting antioxidation via microRNA-101-3p/Nrf2 pathway, Aging 11 (21) (2019) 9295–9309, https://doi.org/10.18632/aging.102348.
[14] R.I. McLachlan, E. Rajpert-De Meyts, C.E. Hoei-Hansen, D.M. de Kretser, N.E. Skakkebaek, Histological evaluation of the human testis–approaches to optimizing the clinical value of the assessment: mini review, Hum. Reprod. 22 (1) (2007) 2–16, https://doi.org/10.1093/humrep/del279.
[15] Q. Lin, S. Weis, G. Yang, Y.H. Weng, R. Helston, K. Rish, et al., Heme oxygenase-1 protein localizes to the nucleus and activates transcription factors important in oxidative stress, J. Biol. Chem. 282 (28) (2007) 20621–20633, https://doi.org/10.1074/jbc.M607954200.
[16] M. Cellat, C.T. İşler, A. Uyar, M. Kuzu, T. Aydın, M. Etyemez, et al., Protective effect of Smilax excelsa L. pretreatment via antioxidant, anti-inflammatory effects, and activation of Nrf-2/HO-1 pathway in testicular torsion model, J. Food Biochem. 46 (8) (2022) e14161, https://doi.org/10.1111/jfbc.14161.
[17] O.O. Oduwole, I.T. Huhtaniemi, M. Misrahi, The roles of luteinizing hormone, follicle-stimulating hormone and testosterone in spermatogenesis and folliculogenesis revisited, Int. J. Mol. Sci. 22 (23) (2021), https://doi.org/10.3390/ijms222312735.
[18] F. Davoodi, S. Taheri, A. Raisi, A. Rajabzadeh, A. Zakian, M.H. Hablolvarid, et al., Leech therapy (Hirudo medicinalis) attenuates testicular damages induced by testicular ischemia/reperfusion in an animal model, BMC Vet. Res. 17 (1) (2021) 256, https://doi.org/10.1186/s12917-021-02951-5.
[19] S. Taheri, F. Davoodi, A. Raisi, A. Zakian, A. Rajabzadeh, M.H. Hablolvarid, et al., Co-administration of Salvia miltiorrhiza and verapamil inhibits detrimental effects of torsion/detorsion on testicular tissue in rats, Andrologia 53 (6) (2021) e14049, https://doi.org/10.1111/and.14049.
[20] M. Jafarova Demirkapu, S. Karabag, H.M. Akgul, C. Mordeniz, H.R. Yananli, The effects of etomidate on testicular ischemia reperfusion injury in ipsilateral and contralateral testes of rats, Eur. Rev. Med. Pharmacol. Sci. 26 (1) (2022) 211–217, https://doi.org/10.26355/eurrev_202201_27770.
[21] L. Li, Y. Hao, Y. Zhao, H. Wang, X. Zhao, Y. Jiang, et al., Ferroptosis is associated with oxygen-glucose deprivation/reoxygenation-induced Sertoli cell death, Int. J. Mol. Med. 41 (5) (2018) 3051–3062, https://doi.org/10.3892/ijmm.2018.3469.
[22] Y. He, H. Li, J. Yao, H. Zhong, Y. Kuang, X. Li, et al., HO-1 knockdown upregulates the expression of VCAM-1 to induce neutrophil recruitment during renal ischemia-reperfusion injury, Int. J. Mol. Med. 48 (4) (2021), https://doi.org/10.3892/ijmm.2021.5018.